

# Localization-Based Resource Selection Schemes for Network-Controlled LTE-V2V

Giammarco Cecchini, Alessandro Bazzi, Barbara M. Masini, Alberto Zanella  
CNR-IEIIT, Bologna, Italy

Email: {giammarco.cecchini, alessandro.bazzi, barbara.masini, alberto.zanella}@ieiit.cnr.it

**Abstract**—3GPP has recently introduced new features to the long term evolution (LTE) cellular technology enabling direct vehicle-to-vehicle (V2V) communications, also known as LTE-V2V. This new technology aims at supporting a large number of applications, most of them based on the broadcasting of periodic messages by all vehicles to inform the neighborhood about relevant information such as vehicle position, direction, and speed. Since resources are inevitably scarce and vehicles move relatively fast, the optimization of the LTE resource allocation represents a crucial topic of research. In this paper, we focus on network-controlled resource management based on the knowledge of the position of vehicles by the network and we propose an algorithm based on the concept of reuse distance. Apart from the ideal case where the position is perfectly estimated, the performance in terms of blocking rate, error rate and packet reception ratio is evaluated also in realistic cases where the position is known with some inaccuracy. In addition, a margin to the reuse distance is proposed to reach the maximum communication distance with a given quality of service. Results, obtained through simulations in a realistic highway scenario, show that there are minimum differences in terms of blocking rate between the different positioning errors, while there might be a significant worsening of the error rate. In addition, the use of an optimized margin is shown with the aim of improving the maximum communication distance of up to 20%.

## I. INTRODUCTION

Vehicles will be soon equipped with devices able to provide connectivity among them and other surrounding objects, enabling several innovative applications and services. Among other implications, such devices aim at reducing the number of car accidents and the emergency response time, at improving the management of traffic congestions and also to foster the future cooperative autonomous driving [1], [2].

At the time of writing, the only complete wireless standard specifically designed for vehicular networks is represented by WAVE/IEEE 802.11p in the US and the corresponding ETSI ITS-G5 in Europe, which are protocol suites based on the Wi-Fi standard specifically amended for the vehicular environment. However, some drawbacks are continuously delaying the time when vehicles will integrate such devices on board. First of all, the fully decentralized and collision based MAC protocol does not give guarantees on the quality of service and opens debates about its functioning in high density scenarios. Other issues are the critical deployment of road side units due to the high costs, the absence of any plan for technology improvement and concerns about security and network maintenance. At last, but probably above all, there is a lack of clarity of the business model: since no operator

is meant to be involved, car makers do not get direct value, and the user would take benefit only when a large if not full penetration is reached.

On the other hand, cellular networks have recently shown huge performance improvements, especially regarding capacity, latency and reliability. The latest cellular standard, long term evolution (LTE), is currently available in almost all countries, quickly growing and offering better performance, thus making the entire system able of being easily upgraded to support new use cases. LTE appears indeed capable of satisfying the delay requirements for most of the vehicular applications, although its scalability might be an issue if the infrastructure must convey all sent and received messages [3].

The idea of employing LTE for the vehicular network deployment found a new opportunity with the introduction of device-to-device (D2D) in Release 12, frozen in March 2015, which enabled direct communications between devices. With D2D, vehicles directly communicate, allowing spatial resource reuse that can lead to significant performance improvements. For this reason, the on-going LTE Release 14, which was expected to be frozen within June 2017, is thus expanding the concept of cellular network to specifically address vehicle-to-vehicle (V2V) and, more in general, vehicle-to-everything (V2X) communications [4]–[7]. LTE-V2V constitutes a valid alternative to standalone wireless short range communications, thanks to the use of more efficient PHY and MAC layers, to the presence of an already widespread infrastructure, to continuously evolving specifications, and to more clear business models to push it on the vehicles.

One of the main openly debated issues in LTE-V2V is the resource scheduling for the cooperative awareness service, which is the transmission of periodic messages, called cooperative awareness messages (CAMs) by ETSI, from all vehicles to the surrounding nodes to provide updated vision of the neighborhood and allow coordinated operations. Specifically, how to optimally reuse resources and which is the impact of the designed algorithm on the achieved performance are still under study. For example, in [8], [9] the authors investigate optimal resource allocations when the vehicles share resources with normal cellular users, while in [10] a distribute algorithm for autonomous resource selection is proposed.

In this work, we focus on the network-controlled case, where the network assigns the resources to be used based on its view of the network and. Coherently with the specifications, we assume a dedicated carrier for V2V communications.

In particular, in this paper we:

- propose an algorithm for in-coverage resource allocation based on the concept of reuse distance;
- define the blocking rate, the error rate and the packet reception ratio as metrics to determine the performance of the allocation algorithm;
- evaluate the impact of possible inaccuracies on the position of vehicles known by the network;
- introduce the application of a margin to the reuse distance in order to achieve a given quality of service.

Results are obtained by the simulation of a realistic highway scenario. Concerning the inaccuracies, we consider two cases: one where the coordinates of vehicles are estimated with some error (e.g., obtained by uplink time difference of arrival (UTDOA)), and the other where positions are updated with a reduced frequency (e.g., based on global navigation satellite system (GNSS) information periodically provided by each vehicle in uplink).

The paper is organized as follows: in Section II, a brief overview of the LTE-V2V PHY and MAC layers is presented; in Section III, the examined scenario and the main assumptions are introduced; in Section IV the simulation settings are discussed and numerical results are provided; finally, in Section V our conclusions are drawn.

## II. LTE-V2V PHY AND MAC LAYERS

3GPP has recently published the first version of LTE Release 14, which updates the cellular standard to support V2X communications. Being based on the uplink settings of LTE, at the PHY layer it adopts orthogonal frequency division multiplexing (OFDM) and at the MAC layer it exploits single carrier frequency division multiple access (SC-FDMA), with the available bandwidth subdivided into orthogonal contiguous subcarriers. This access scheme is implemented in order to limit transmitted signal fluctuations, achieving a lower value of the peak to average power ratio (PAPR) compared to orthogonal frequency division multiple access (OFDMA) conventionally used for the downlink, which translates in a lower distortion due to non-linearity at the amplifier.

According to the LTE specifications, in the time domain data are organized in frames having 10 ms duration. Each frame is then divided into 10 subframes of 1 ms. Each subframe is further divided into two slots, each of 0.5 ms duration. In the frequency domain, 12 consecutive and equally spaced subcarriers and one time slot compose a resource block (RB). Resources are defined on a subframe basis, hence two consecutive RBs constitute the smallest element of resource allocation assigned by the base station scheduler, which is made of 12 subcarriers in the frequency domain and 14 OFDM symbols in the time domain.

Release 14 adds some modifications to the LTE subframe in order to optimize it for V2V communications, where nodes move fast and often transmit periodically. More precisely, like in basic D2D communications (also called Sidelink Mode 1 and Mode 2) the last symbol of the mentioned 14 OFDM symbols is left unused for timing adjustments and Tx-Rx

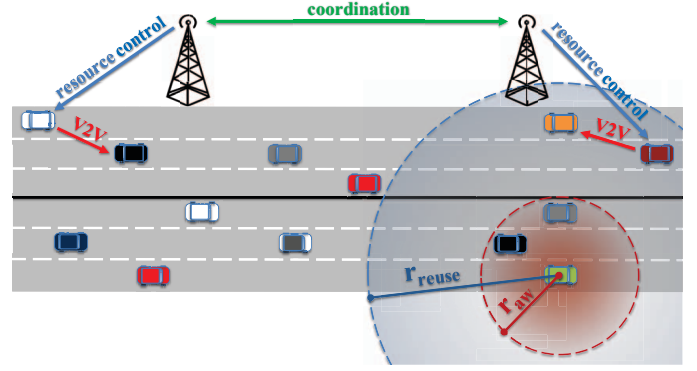


Fig. 1. Network-controlled highway scenario.

switching and two OFDM symbols are used as demodulation reference signal (DMRS). In LTE-V2V, to counterbalance the high Doppler spread that arises in high mobility scenario, two further DMRS symbols are added; hence, only 9 OFDM symbols per subframe are available for carrying data [4].

The number of data bits that can be carried by the couples of RBs or, equivalently, the number of RBs needed to carry a message depend on the adopted modulation and coding scheme (MCS), as carefully detailed in [11]. The same choice also impacts on the minimum signal to noise and interference ratio (SINR) required at the receiver and consequently on the maximum communication and reuse ranges (defined in Section III-A).

Regarding the resource allocation procedures, LTE Release 14 addresses both network-controlled and autonomous schemes. In the former, the scheduling and interference management of V2V traffic is assisted by evolved NodeBs (eNBs) (Sidelink Mode 3) via control signalling. It is assumed that the scenario is fully covered by one or more eNBs which, through coordination and synchronization, will assign the resources being used for V2V communications in a dynamic manner. In the latter, LTE-V2V traffic is allocated based on distributed algorithms (Sidelink Mode 4) implemented between the vehicles. A mechanism based on sensing with semi-persistent transmission is introduced to optimize the use of the channel by enhancing resource separation between transmitters that are using overlapping resources.

In this work, we focus on network-controlled resource allocations (Sidelink Mode 3), whereas autonomous resource allocations will be subject of future work.

## III. PROBLEM FORMULATION

### A. Scenario

We focus on a highway scenario with vehicles travelling on multiple lanes and in both directions. Since we are considering the network-controlled allocation, we assume full LTE coverage, with multiple synchronized eNBs. Exploiting their knowledge on vehicle positions and propagation characteristics, the eNBs allocate the resources to guarantee the required quality of service, but reusing the same resources within the cells as much as possible to maximize the network capacity.

Each vehicle aims at transmitting a beacon message periodically, with constant generation period  $T_{bc}$  and size  $B_{bc}$ . Resources are allocated on a semi-persistent basis, that is the same RBs are periodically assigned until a re-allocation is performed. The message is intended to be received by all the neighbors within a given distance, denoted awareness range  $r_{aw}$  and defined by design.

The allocation procedure described later is based on the definition of the minimum reuse distance  $r_{reuse}$ , which is the minimum distance at which the same resource can be used by a different transmitter without affecting those receivers that are in the awareness range. Following [11], the reuse range can be calculated as

$$r_{reuse} = r_{aw} + \frac{r_{aw}}{\left[ \frac{1}{\gamma_{min}} - \frac{P_{nRB}}{P_{txRB}} \cdot \frac{L_0 \cdot r_{aw}^\beta}{G_r} \right]^{\frac{1}{\beta}}} \quad (1)$$

where  $r_{aw}$  is the required awareness range,  $\gamma_{min}$  is the minimum SINR necessary to correctly decode the message,  $P_{txRB}$  is the transmission power per RB,  $P_{nRB}$  the noise power over a RB,  $L_0$  the path loss at 1 m,  $\beta$  the loss exponent, and  $G_r$  the antenna gain at the receiver. Calculations are based on the assumption that the interference is mostly due to the contribution of the nearest interferer.

The scenario is exemplified in Fig. 1.

### B. Resource Management Algorithm

Given a new vehicle requiring the allocation of resources, the network first individuates those RBs that are used by vehicles in its awareness range; since standard half duplex (HD) devices are considered (thus the vehicle either transmits or receives in a subframe), all the RBs of a subframe where at least one RB is used to receive a beacon cannot be allocated. Furthermore, the RBs used by the vehicles outside the awareness but within the reuse range are also marked as not available. If the remaining RBs are not enough for the transmission of the beacon, then the vehicle is blocked until the next beacon is generated and a new attempt is performed. Otherwise, the required RBs are randomly chosen among those remained available with the constrain to use RBs of the same subframe, if possible (or the less possible subframes).

In principle, based on the position of vehicles and the calculation of the reuse range, the network allocates the resources with minimum probability of errors. However, the continuous movements of the vehicles in the scenario cause the performed allocations to quickly become outdated, thus requiring frequent reassignments. In the proposed algorithm, reallocations are performed as soon as at least one error in reception occurs due to poor SINR ( $\gamma < \gamma_{min}$ ).

Furthermore, the position known at the network side is realistically affected by some inaccuracy. In particular, two effects could be observed:

- *positioning error*: the localization is achieved with some error;
- *update delay*: the position is known only every some time interval, thus causing a delay in the update.

TABLE I  
MAIN INPUTS AND SETTINGS.

Parameter (Symbol)	Value
Simulated time ( $T_{sim}$ )	90 s
Beacon period ( $T_{bc}$ )	100 ms
Beacon size ( $B_{bc}$ )	190 or 300 bytes
Ratio of LTE UL RBs allocated to the service ( $\delta$ )	0.5
Path loss at 1 m ( $L_0$ )	47.86 dB
Loss exponent ( $\beta$ )	2.75
Antenna gain at the receiver ( $G_r$ )	3 dB
Noise power over an RB ( $P_{nRB}$ )	-110 dBm
Channel bandwidth ( $B_w$ )	10 MHz
Modulation and coding scheme (MCS)	5
Equivalent radiated power ( $P_{tx}$ )	23 dBm
Required awareness range ( $r_{aw}$ )	$\in [50 \div 275]$
UTDOA positioning: 95th-percentile of error	100 m
GNSS positioning: update delay	2 s

The considered models for the positioning inaccuracies are detailed in the following subsection.

### C. Considered Localization Methods

To provide two examples of possible localization methods possibly affected by different inaccuracies, hereafter we simulate the use of UTDOA [12] and the uplink collection of data from the GNSS modules mounted on vehicles [13].

**UTDOA and positioning error.** UTDOA [12], introduced in Release 11 of LTE, allows the estimation of the position of each node avoiding the waste of resources caused by dedicated signalling on the uplink. Multiple synchronized eNBs measure the sounding reference signal (SRS) transmitted by the UE and calculate the terminal position through multilateration; at least 3 eNBs are required to solve for two lateral coordinates of the UE and the receiver clock bias. The accuracy of UTDOA depends on different factors, such as the signal bandwidth, the number of involved eNBs and the network timing synchronization. According to [14], UTDOA performance with 5 detecting eNBs could almost meet the FCC satellite technology positioning requirements of 50 m for 67% of time and 100 m for 95% of time. For this reason, we model the localization accuracy at the network side by adding an error to the real positions of vehicles. The positioning error is generated for each vehicle independently at each beacon period, with the norm of the error vector modeled as the absolute value of a Gaussian random variable with zero mean and standard deviation  $\sigma_{pos} = 100 \text{ m}/1.96 \simeq 51.02 \text{ m}$ . The angle of the error is uniformly distributed between  $[0, 2\pi]$ . Positions are updated at each beacon period.

**GNSS and update delay.** An alternative way for the localization of vehicles consists in assuming that each vehicle uses a GNSS device and communicates the information to the network through an uplink control channel. According to [13], in such case nodes should periodically report their GNSS estimated coordinates at the eNB within an interval of 2 s. Based on this requirement, we model this localization method by updating the knowledge of vehicle position at the network side every 2 s (for each vehicle, the instant of the first localization update is randomly chosen to avoid that all vehicles are updated at the same time). The positioning error

TABLE II  
REQUIRED AWARENESS RANGE VS. MINIMUM REUSE RANGE.

$r_{aw}$	$r_{reuse}$ ( $B_{bc}=190$ bytes)	$r_{reuse}$ ( $B_{bc}=300$ bytes)	avg. neighbors $\pm$ std. deviation
25 m	60 m	61 m	$4.94 \pm 2.41$
50 m	121 m	122 m	$12.69 \pm 4.86$
75 m	182 m	184 m	$19.40 \pm 6.75$
100 m	244 m	247 m	$25.82 \pm 8.33$
125 m	308 m	310 m	$31.98 \pm 9.66$
150 m	375 m	376 m	$38.07 \pm 10.74$
175 m	446 m	446 m	$44.11 \pm 11.53$
200 m	524 m	521 m	$50.12 \pm 12.13$
225 m	615 m	605 m	$56.03 \pm 12.55$
250 m	731 m	703 m	$61.87 \pm 12.55$
275 m	909 m	831 m	$67.67 \pm 13.15$

is instead assumed to be negligible thanks to the capabilities of modern GNSS devices. The possible overhead introduced by the periodic uplink report of the coordinates is beyond the scope of this paper.

#### IV. NUMERICAL RESULTS

Results are achieved through simulations, exploiting the LTEV2Vsim simulator [15], [16] in a realistic highway scenario and comparing ideal positioning to UTDOA and GNSS. The main input and setting parameters are hereafter briefly described and summarized in Table I.

##### A. Main Settings and Observed Outputs.

**Settings.** The scenario corresponds to a traffic trace of a congested highway scenario of approximately 16 km, with 2000 average vehicles distributed over 3 lanes per travel direction [17]. Vehicles move with an average speed of nearly 50 km/h and a standard deviation around 3 km/h. The simulated time  $T_{sim}$  is set to 90 s.

All devices are assumed to adopt an MCS equal to 5, being it among the best choices as discussed in [11]. We evaluated the performance with two different beacon sizes that can be commonly found in literature: 190 and 300 bytes (e.g., [18]). The portion of LTE RBs dedicated to the cooperative awareness V2V service  $\delta$  is assumed equal to 0.5 of a 10 MHz channel. With these settings, the number of available beacon resources (BRs), which corresponds to the number of beacons that can be allocated per beacon period, is equal to 100 when  $B_{bc} = 190$  bytes and to 50 when  $B_{bc} = 300$  bytes. With an equivalent radiated power per beacon  $P_{tx} = 23$  dBm and following the computations reported in [11], the equivalent radiated power per RB  $P_{txRB}$  is nearly 7.4 dBm when  $B_{bc} = 190$  bytes, corresponding to a maximum awareness range of 307 m, and approximately 8.51 dBm when  $B_{bc} = 300$  bytes, giving a maximum awareness range of 330 m. Example ranges are reported in Table II, together with the average number of neighbors.

**Outputs.** The following key performance indicators (KPIs) are considered:

- the *average blocking rate (ABR)*, computed as the ratio between the number of blocked transmitters due to un-

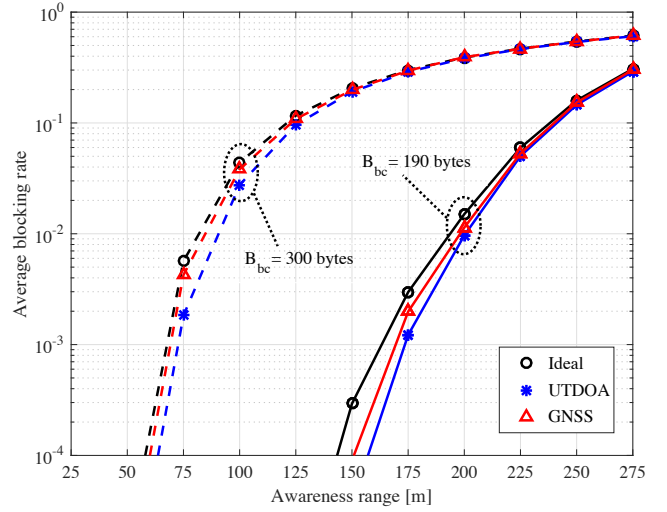


Fig. 2. Average blocking rate vs. awareness range, comparing the different positioning methods with  $B_{bc} = 190$  bytes (solid lines) or  $B_{bc} = 300$  bytes (dashed lines).

availability of BRs and the total number of vehicles in the scenario;

- the *average error rate (AER)*, defined as the ratio between the number of not correctly decoded beacons and the number of beacons that were expected to be received.
- the *packet reception ratio (PRR)*, given by the ratio between the number of successfully received beacons and the sum of the number of neighbors of all vehicles. It can be noted that the PRR considers both blocked vehicles and errors at the receivers, thus it somehow summarizes the two previous metrics.

##### B. Performance Evaluation

Fig. 2 shows the ABR as a function of the awareness range for the two values of beacon size  $B_{bc}$ ; three curves are shown for each value of  $B_{bc}$ : ideal positioning (Ideal), positioning with UTDOA (UTDOA), and positioning with GNSS (GNSS). The figure shows that inaccuracies due to realistic localization systems have a minor effect on the blocking rate, with the ideal case resulting in slightly higher values. As expected, the case with  $B_{bc} = 300$  bytes provides a larger blocking rate and allows only a limited value of  $r_{aw}$  (e.g. the maximum  $r_{aw}$  for a blocking rate not exceeding  $10^{-2}$  is only around 75 m). On the contrary, with  $B_{bc} = 190$  bytes the value of the blocking rate is less than  $10^{-2}$  until values of  $r_{aw}$  higher than 175 m.

A different behavior can be observed in Fig. 3, which shows the AER as a function of the awareness range with the same system parameters of Fig. 2. First of all, it can be noted that the curves are in general not monotonic with  $r_{aw}$ ; on one hand, increasing  $r_{aw}$  the vehicle movements are shorter compared to the ranges, thus the error rate tends to reduce; on the other hand, the error rate tends to increase for large values of  $r_{aw}$  due to a noticeable increase of the average number of neighbors, which consequently results in a higher probability that the

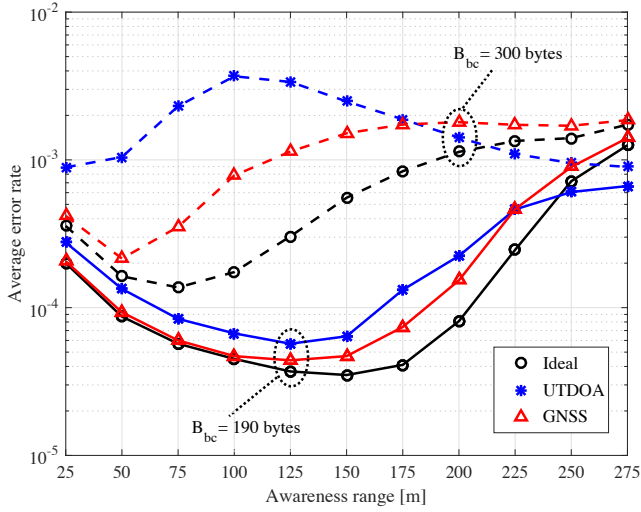


Fig. 3. Average error rate vs. awareness range, comparing the different positioning methods with  $B_{bc} = 190$  bytes (solid lines) or  $B_{bc} = 300$  bytes (dashed lines).

same resources are used by vehicles which are near to the reciprocal reuse range.

In addition, it is evident that the positioning error plays a significant role in this case and that the use of UTD OA provides the worst performance for both values of  $B_{bc}$ . In particular, in the ideal case, with  $B_{bc} = 300$  bytes the error rate goes from approximately  $10^{-4}$  ( $r_{aw} = 75$  m) to almost  $10^{-3}$  when  $r_{aw}$  reaches 200 m, while with  $B_{bc} = 190$  bytes it remains always below  $10^{-4}$  for values of  $r_{aw}$  between 50 to 200 m. Adopting GNSS, the error rate tends to be generally higher, especially when the resources are almost saturated and the reuse range is small, that is with  $B_{bc} = 300$  bytes and  $r_{aw} \leq 125$  m. Finally, when UTD OA is exploited, the worsening becomes remarkable. This behavior is caused by the fact that the resource reallocation due to a decoding error is always performed by the network on the basis of a different random estimation of the positions of vehicles, which makes errors occur more frequently.

Finally, Fig. 4 shows that there are no substantial differences in the packet reception ratio achieved with the three positioning methods. This is due to the fact that in all the conditions the losses due to blocked vehicles impact much more than the reception errors.

### C. Applying a Margin to the Reuse Distance

The results shown from Fig. 2 to Fig. 4 suggest that the performance of the system can be limited by just one of the two metrics (ABR and AER) with the given settings; e.g., the blocking rate is often unacceptably high, even if the value of  $r_{aw}$  is sufficiently low to guarantee a tolerable error rate. For this reason, we introduce a new parameter to balance the ABR and the AER in order to achieve an adequate quality of service (QoS), fixing a minimum threshold of the PRR, which depends on both the other two metrics, as previously mentioned.

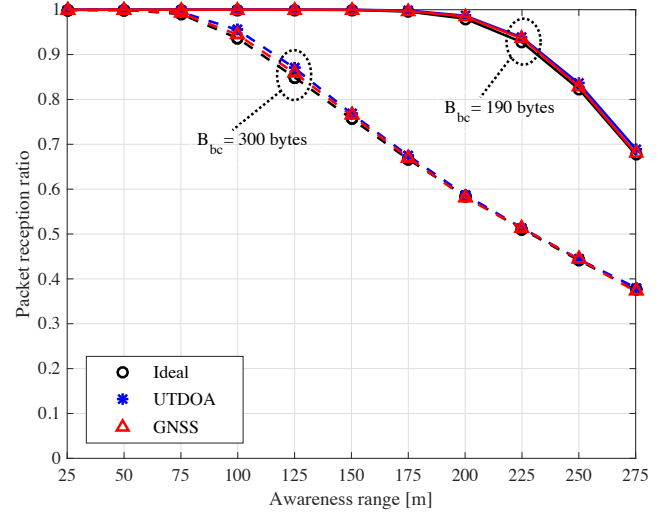


Fig. 4. Packet reception ratio (PRR) vs. awareness range, comparing the different positioning methods with  $B_{bc} = 190$  bytes (solid lines) or  $B_{bc} = 300$  bytes (dashed lines).

Let us focus on a generic  $r_{aw}$  and the consequent  $r_{reuse}$ . Compared to the described allocation procedure, if the allocation is performed with the same algorithm, but applying a reuse distance larger than  $r_{reuse}$ , the blocking rate increases (on average, more vehicles share the same resources), while the error rate reduces (on average, a larger distance is imposed to vehicles using the same resources). Clearly, the opposite is true applying a reuse distance smaller than  $r_{reuse}$ .

At this point, we introduce the parameter  $r_m$ , hereafter denoted as *reuse margin*, to be added to the reuse distance calculated in (1), with the scope to control the blocking versus error rate trade-off. More specifically, the allocation is based on a modified reuse distance  $r_{reuse}^*$  set as

$$r_{reuse}^* \triangleq r_{reuse} + r_m. \quad (2)$$

Please observe that  $r_m$  can also be negative and it must be  $r_m > -r_{reuse}$ .

With the described modification to the algorithm and assuming a target  $PRR \geq 0.99$ , in Fig. 5 the maximum achievable  $r_{aw}$  is shown varying  $r_m$  for both the positioning errors (UTD OA and GNSS) with  $B_{bc} = 190$  bytes. Starting from a margin  $r_m = -160$  m and increasing it up to  $r_m = 40$  m, we observe an increase of the maximum  $r_{aw}$  and then a slow decrease above a given  $r_m$ , which is different in the two cases. In both, an excessively negative margin implies that the maximum  $r_{aw}$  is limited by a high error rate, whereas a large positive margin causes the maximum  $r_{aw}$  to be limited by a high blocking rate. Please observe that, since both UTD OA and GNSS have shown to behave similarly in terms of blocking rate (Fig. 2), the maximum  $r_{aw}$  is almost the same for values of the margins above -80 m, where the performance is mostly limited by the blocking rate.

In the GNSS case, a peak value of  $r_{aw}$  of nearly 220 m (about 20% more than without the application of the margin) is achieved with a negative margin between -120 and -100 m.



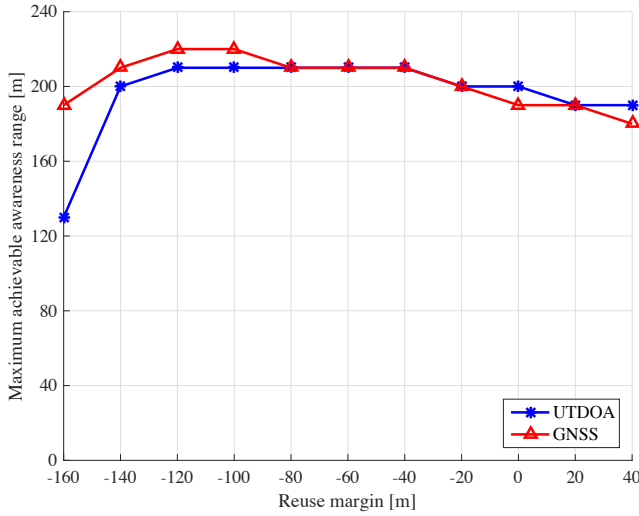


Fig. 5. Maximum awareness range vs. reuse margin to achieve a PRR  $\geq 0.99$  with  $B_{bc} = 190$  bytes.

In that case, an error rate significantly lower than  $10^{-2}$  has been shown in Fig. 3 and the performance without the margin is limited by the blocking rate. The use of a negative margin thus allows to reduce the blocking rate at the expense of an acceptable increase of the error rate.

In the UTDOA case, a peak value of  $r_{aw}$  around 210 m, which is a little less than the one achieved in the GNSS case, is obtained with a negative margin between -120 and -40 m. Fig. 5 confirms that, in this case, the error rate has more impact on the PRR for excessively negative values of the margin. A higher margin gives less errors at the expense of more blocking events.

## V. CONCLUSION

In this paper, we focused on LTE-V2V and discussed the network-controlled resource management of beacon transmission for cooperative awareness, based on the knowledge of the position of vehicles and on the reuse distance. The proposed resource allocation algorithm was checked via simulations by considering some use cases: i) the case where the position is perfectly known, ii) the presence of a positioning error such as if UTDOA is used to estimate the position of vehicles, and iii) an infrequent update of the positions such as if GNSS data is collected and sent in uplink by the vehicles. The results showed that, although the blocking rate does not vary so much according to the localization technique adopted, the error rate strongly depends on that. In particular, a Gaussian positioning error with variance of approximately 50 m and random direction, assumed for UTDOA, leads to a high value of the error rate, suggesting that the accuracy of the localization is more important than the frequency of the update (GNSS). In addition, we added a margin to the reuse distance to optimize the trade-off between the blocking and the error rates, achieving a required QoS in the packet reception ratio.

Results highlighted that the optimal value of the margin, which depends on the considered localization technique, can increase, even by 20%, the achievable communication range for the investigated service.

## REFERENCES

- [1] M. Rondinone, J. Gozalvez, J. Leguay, and V. Conan, "Exploiting context information for v2x dissemination in vehicular networks," in *2013 IEEE 14th International Symposium on "A World of Wireless, Mobile and Multimedia Networks" (WoWMoM)*, June 2013, pp. 1–9.
- [2] L. Hobert, A. Festag, I. Llatser, L. Altomare, F. Visintainer, and A. Kovacs, "Enhancements of v2x communication in support of cooperative autonomous driving," *IEEE Communications Magazine*, vol. 53, no. 12, pp. 64–70, Dec 2015.
- [3] G. Araniti, C. Campolo, M. Condoluci, A. Iera, and A. Molinaro, "LTE for vehicular networking: a survey," *IEEE Communications Magazine*, vol. 51, no. 5, pp. 148–157, May 2013.
- [4] 3GPP: Initial cellular V2X standard completed. Accessed on April 2017. [Online]. Available: [http://www.3gpp.org/news-events/3gpp-news/1798-v2x\\_r14](http://www.3gpp.org/news-events/3gpp-news/1798-v2x_r14)
- [5] A. Bazzi, B. M. Masini, A. Zanella, and I. Thibault, "Beaconing from connected vehicles: IEEE 802.11p vs. LTE-V2V," in *2nd International Workshop on Vehicular Networking and Intelligent Transportation Systems (VANETS)*, September 2016.
- [6] H. Seo, K. D. Lee, S. Yasukawa, Y. Peng, and P. Sartori, "LTE evolution for vehicle-to-everything services," *IEEE Communications Magazine*, vol. 54, no. 6, pp. 22–28, June 2016.
- [7] S. H. Sun, J. L. Hu, Y. Peng, X. M. Pan, L. Zhao, and J. Y. Fang, "Support for vehicle-to-everything services based on LTE," *IEEE Wireless Communications*, vol. 23, no. 3, pp. 4–8, June 2016.
- [8] G. Li, Z. Yang, S. Chen, Y. Li, and P. Yuan, "A traffic flow-based and dynamic grouping-enabled resource allocation algorithm for LTE-D2D vehicular networks," in *2016 IEEE/CIC International Conference on Communications in China (ICCC)*, July 2016, pp. 1–6.
- [9] W. Sun, E. G. Strom, F. Brannstrom, K. C. Sou, and Y. Sui, "Radio resource management for D2D-based V2V communication," *IEEE Transactions on Vehicular Technology*, vol. 65, no. 8, pp. 6636–6650, Aug 2016.
- [10] J. Yang, B. Pelletier, and B. Champagne, "Enhanced autonomous resource selection for LTE-based V2V communication," in *2016 IEEE Vehicular Networking Conference (VNC)*, Dec 2016.
- [11] A. Bazzi, B. M. Masini, and A. Zanella, "How many vehicles in the LTE-V2V awareness range with half or full duplex radios?" in *15th edition of International Conference on Intelligent Transport Systems (ITS) Telecommunications (ITST 2017)*, Warsaw, May 2017.
- [12] 3GPP, "Technical specification group radio access network; evolved universal terrestrial radio access network (E-UTRAN); stage 2 functional specification of user equipment (UE) positioning in E-UTRAN (release 14)," *3GPP TS 36.305 V14.1.0*, March 2017.
- [13] —, "Technical specification group radio access network; evolved universal terrestrial radio access network (E-UTRAN); requirements for support of assisted global navigation satellite system (A-GNSS) (release 14)," *3GPP TS 36.171 V14.0.0*, March 2017.
- [14] —, "UTDOA performance with SRS interference cancellation," *Alcatel-Lucent Shanghai Bell, 3GPP TSG RAN WG1 R1-105997, Jacksonville, FL, U.S.A.*, November 2010.
- [15] G. Cecchini, A. Bazzi, B. M. Masini, and A. Zanella, "LTEV2Vsim: An LTE-V2V simulator for the investigation of resource allocation for cooperative awareness," in *5th IEEE International Conference on Models and Technologies for Intelligent Transportation Systems (MT-ITS 2017)*, Naples (Italy), June 2017.
- [16] Web page of LTEV2Vsim. Accessed on April 2017. [Online]. Available: <http://www.wcsg.ieit.cnr.it/products/LTEV2Vsim.html>
- [17] A. Bazzi, B. M. Masini, A. Zanella, and A. Calisti, "Visible light communications as a complementary technology for the internet of vehicles," *Elsevier Computer Communications, Multi-radio, Multi-technology, Multi-system Vehicular Communications*, 2016.
- [18] "Details of sensing for V2V," *Qualcomm Incorporated, 3GPP TSG RAN WG1 R1-163032, Busan, Korea*, April 2016.